Orthogonal frequency division multiplexing with power distribution index modulation

A. T. Dogukan and E. Basar ✉

Orthogonal frequency division multiplexing with index modulation (OFDM-IM) is a promising multicarrier transmission technique that exploits both conventional modulation and the indices of active subcarriers for data transmission. In this letter, we propose OFDM with power distribution index modulation (OFDM-PIM) where a unique power distribution technique is applied to index modulated subcarriers. Furthermore, we propose OFDM with in-phase/quadrature PIM (OFDM-I/Q-PIM) which performs the same power distribution process on the real and imaginary parts of the data symbols, independently. Average bit error performances (ABEP) of OFDM-PIM and OFDM-I/Q-PIM are obtained and the superiority of the proposed schemes over reference schemes is demonstrated via extensive computer simulations.

Introduction: Orthogonal frequency division multiplexing (OFDM) is a very popular multicarrier transmission system which has been used in many standards such as IEEE 802.11x and LTE. Even though OFDM is not relatively new, it still maintains its importance for state-of-the-art wireless communication technologies. OFDM is the selected waveform for 5G wireless networks thanks to its several advantages such as simplicity, compability, and robustness to frequency selective fading. In the literature, numerous studies have been done by researchers to enhance the performance of OFDM. A very simple diversity-enhancing scheme called repetition coded OFDM (RC-OFDM) [1] is proposed where repetition coding is applied to OFDM subcarriers to improve its error performance. However, it is difficult to achieve high spectral efficiencies with RC-OFDM since it exploits multiple subcarriers (frequency resources) for the transmission of the same data symbol.

Index modulation (IM) [2], which employs the indices of transmit entities such as antennas and time slots, has been emerged as a promising digital modulation concept. OFDM-IM [3] is proposed by combining OFDM and IM in an efficient and clever manner. In OFDM-IM, information bits are transmitted by both M-ary signal constellations and subcarrier indices. In contrast to conventional OFDM, OFDM-IM, which is capable of adjusting subcarrier activation ratio, provides an interesting trade-off between spectral and performance efficiency. Many studies have been carried out to improve the performance of OFDM-IM. OFDM-IM using coordinate interleaving (CI-OFDM-IM) [4], which transmits the real and imaginary parts of the data symbols over different active subcarriers, is proposed to provide a diversity gain. OFDM with in-phase/quadrature IM (OFDM-I/Q-IM) [5] is proposed to transmit additional index bits by appliying IM independently to real and imaginary parts of the data symbol. Owing to the flexible transceiver structure of OFDM-IM, numerous schemes [6, 7, 8] have been recently proposed to provide solutions for the requirements of 5G wireless services such as ultra-reliable low-latency communication (URLLC) and enhanced mobile broadband (eMBB).

Against this background, we propose OFDM with power distribution index modulation (OFDM-PIM) where information bits are transmitted by both M-ary signal constellations and subcarrier indices along with high/low power levels. In OFDM-PIM, each data symbol is distributed over two subcarriers with high/low power levels. To further increase the number of bits conveyed by IM, OFDM with in-phase/quadrature PIM (OFDM-I/Q-PIM), which extends OFDM-PIM to in-phase and quadrature dimensions, is proposed. In OFDM-I/Q-PIM, the subcarrier indices for high/low power levels are determined twice for both real and imaginary parts of the data symbols. The derivation of the average bit error probability (ABEP) and the power level selection strategy are given for OFDM-PIM and OFDM-I/Q-PIM. It is revealed via computer simulations that OFDM-PIM and OFDM-I/Q-PIM outperform the their counterparts.

System model of OFDM-PIM: The transmitter structure of OFDM-PIM is given in Fig. 1. A total number of m bits are conveyed with the transmission of each OFDM block. These bits are split into G groups. Each group contains $p = m/G = p_1 + p_2$ bits and these bits form a subblock with length $n = N/G$, where N is the size of the fast Fourier transform (FFT). For the creation of gth

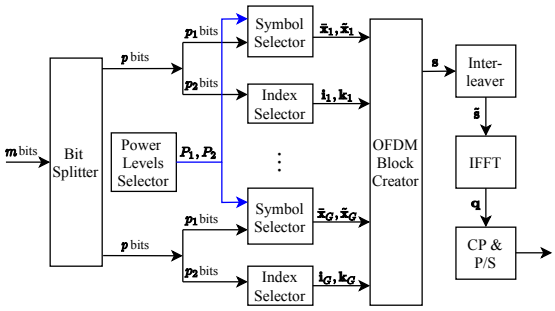

Fig. 1. Transmitter structure of OFDM-PIM.

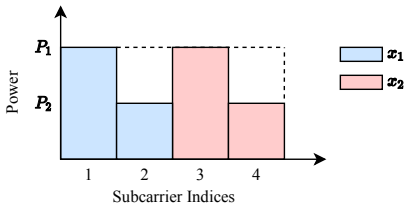

Fig. 2. Power distribution for the example subblock given in (2).

subblock $\mathbf{s}_g$, firstly, $p_1 = \frac{n}{2}\log_2(M)$ bits determine the data symbols $\mathbf{x}_g = [x_g(1), x_g(2), \cdots, x_g(n/2)]$, $g = 1, \cdots, G$ from the M-ary signal constellation. The average power of the signal constellation is normalized to unity. We define two power levels, high (P_1) and low (P_2), where $P_1 > P_2$ and $P_1 + P_2 = 2$ under normalized subcarrier powers. The selection strategy of P_1 and P_2 is given in the following section. Secondly, $p_2 = \lfloor \log_2 \binom{n}{n/2} \rfloor$ bits determine the indices of high power subcarriers $\mathbf{i}_g = [i_g(1), i_g(2), \cdots, i_g(n/2)]$ using combinatorial method as in [3]. The remaining subcarrier indices are assigned a low power and are represented as $\mathbf{k}_g = [k_g(1), k_g(2), \cdots, k_g(n/2)]$. Then, the data symbols vector $\mathbf{x}_g$ is multiplied with $\sqrt{P_1}$ and $\sqrt{P_2}$ and the new data symbols vectors $\bar{\mathbf{x}}_g = \sqrt{P_1}[x_g(1), x_g(2), \cdots, x_g(n/2)]$ and $\tilde{\mathbf{x}}_g = \sqrt{P_2}[x_g(1), x_g(2), \cdots, x_g(n/2)]$ are obtained. The entries of $\bar{\mathbf{x}}_g$ and $\tilde{\mathbf{x}}_g$ are placed into the subblock with the entries of $\mathbf{i}_g$ and $\mathbf{k}_g$, respectively. Consequently, a total number of

$$p = p_1 + p_2 = \frac{n}{2}\log_2(M) + \lfloor \log_2 \binom{n}{n/2} \rfloor, \tag{1}$$

bits are transmitted per subblock. For convenience, we provide an example for the creation of $\mathbf{s}_g$.

Example: Assume that $n = 4$, $M = 4$ with Gray mapping and we transmit the bit sequence of $\{10|00|01\}$. The first $p_1 = 2\log_2(4) = 4$ bits $\{10|00\}$ determine the data symbols as $\mathbf{x}_g = [-1, j]$. Later, the power allocated data vectors are obtained as $\bar{\mathbf{x}}_g = [-\sqrt{P_1}, \sqrt{P_1}j]$ and $\tilde{\mathbf{x}}_g = [-\sqrt{P_2}, \sqrt{P_2}j]$. Then, $p_2 = \lfloor \log_2 \binom{4}{2} \rfloor = 2$ bits $\{01\}$ determine the indices of high power subcarriers as $\mathbf{i}_g = [1, 3]$ and the remaining ones are the indices of low power subcarriers $\mathbf{k}_g = [2, 4]$. Finally, $\mathbf{s}_g$ can be given as:

$$\mathbf{s}_g = [-\sqrt{P_1} \; -\sqrt{P_2} \; \sqrt{P_1}j \; \sqrt{P_2}j]^{\mathrm{T}}, \tag{2}$$

where $(\cdot)^{\mathrm{T}}$ denotes transposition. The power distribution for the example subblock given in (2) is shown in Fig. 2.

By applying the same procedures for all subblocks, the main OFDM block $\mathbf{s} = [\mathbf{s}_1^{\mathrm{T}} \mathbf{s}_2^{\mathrm{T}} \cdots \mathbf{s}_G^{\mathrm{T}}]^{\mathrm{T}}$ is created. A block-type interleaver is performed as in [3] and the interleaved OFDM block $\tilde{\mathbf{s}}$ is obtained. Inverse fast Fourier transform (IFFT) is applied to $\tilde{\mathbf{s}}$ and time-domain OFDM block $\mathbf{q}$ is obtained. Then, a cyclic prefix (CP) of length C is added, parallel-to-serial and digital-to-analog conversions are performed. The resulting signal is transmitted through a T-tap frequency selective Rayleigh fading channel whose elements follow $\mathcal{CN}(0, \frac{1}{T})$ distribution. During the transmission of an OFDM block, we assume that channel remains constant $C > T$. At the receiver, FFT operation is applied. Finally, in the frequency domain, the equivalent input-output relationship can be given as:

$$\tilde{\mathbf{y}} = \tilde{\mathbf{H}}\tilde{\mathbf{s}} + \mathbf{n}, \tag{3}$$

where $\tilde{\mathbf{y}}$, $\tilde{\mathbf{H}} = \mathrm{diag}(\tilde{\mathbf{h}})$, and $\mathbf{n}$ are the received signal vector, the channel matrix, and the noise vector in the frequency domain, respectively, where $\mathrm{diag}(\cdot)$ is diagonalization operation. The distributions of the elements of $\mathbf{h}$ and $\mathbf{n}$ are $\mathcal{CN}(0,1)$ and $\mathcal{CN}(0,N_0)$, respectively, where N_0 is the noise variance. The signal-to-noise ratio (SNR) is defined as $\lambda = E_b/N_0$ where, $E_b = (N+C)/m$ is the average transmitted energy per bit. A block-type deinterleaver is applied to $\tilde{\mathbf{y}}$ and $\tilde{\mathbf{h}}$. We obtain the deinterleaved received signal vector $\mathbf{y}$ and channel vector $\mathbf{h}$.

At the receiver, after removing CP and deinterleaving, received signal and channel vectors are split into G groups and represented as $\mathbf{y} = [\mathbf{y}_1^{\mathrm{T}}\mathbf{y}_2^{\mathrm{T}}\cdots\mathbf{y}_G^{\mathrm{T}}]^{\mathrm{T}}$ and $\mathbf{h} = [\mathbf{h}_1^{\mathrm{T}}\mathbf{h}_2^{\mathrm{T}}\cdots\mathbf{h}_G^{\mathrm{T}}]^{\mathrm{T}}$, respectively. Subblock wise maximum-likelihood (ML) detector is exploited to decode the gth subblock with the set $\mathcal{Z} \in \{\mathbf{z}_1, \mathbf{z}_2, \cdots, \mathbf{z}_{2^p}\}$ that includes all possible subblock realizations:

$$\hat{\mathbf{s}}_g = \arg\min_{\mathbf{z}\in\mathcal{Z}} \|\mathbf{y}_g - \mathbf{H}_g\mathbf{z}\|^2, \tag{4}$$

where $\mathbf{H}_g = \mathrm{diag}(\mathbf{h}_g) \in \mathbb{C}^{n\times n}$. The complexity order of the ML detection can be given as $\mathcal{O}(2^p)$.

Extension to IQ: In order to double the number of bits transmitted by IM, we propose OFDM-I/Q-PIM which applies PIM for both in-phase and quadrature components of the data symbols, separately. After determining data symbols $\bar{\mathbf{x}}_g, \tilde{\mathbf{x}}_g$ as in OFDM-PIM, $\tilde{p}_2 = 2\lfloor \log_2 \binom{n}{n/2} \rfloor$ number of bits determine the subcarrier indices as $\mathbf{i}_g^{\mathcal{I}} = [i_g^{\mathcal{I}}(1), i_g^{\mathcal{I}}(2), \cdots, i_g^{\mathcal{I}}(n/2)]$ and $\mathbf{i}_g^{\mathcal{Q}} = [i_g^{\mathcal{Q}}(1), i_g^{\mathcal{Q}}(2), \cdots, i_g^{\mathcal{Q}}(n/2)]$ for in-phase and quadrature parts of these symbols, respectively. The remaining subcarrier indices are represented as $\mathbf{k}_g^{\mathcal{I}} = [k_g^{\mathcal{I}}(1), k_g^{\mathcal{I}}(2), \cdots, k_g^{\mathcal{I}}(n/2)]$ and $\mathbf{k}_g^{\mathcal{Q}} = [k_g^{\mathcal{Q}}(1), k_g^{\mathcal{Q}}(2), \cdots, k_g^{\mathcal{Q}}(n/2)]$. Then, the entries of $\Re\{\bar{\mathbf{x}}_g\}$ and $\Re\{\tilde{\mathbf{x}}_g\}$ are placed into the subblock with the entries of $\mathbf{i}_g^{\mathcal{I}}$ and $\mathbf{k}_g^{\mathcal{I}}$, respectively, and the entries of $\Im\{\bar{\mathbf{x}}_g\}$ and $\Im\{\tilde{\mathbf{x}}_g\}$ are placed into the subblock with the entries of $\mathbf{i}_g^{\mathcal{Q}}$ and $\mathbf{k}_g^{\mathcal{Q}}$, respectively. Consequently, a total number of

$$\tilde{p} = p_1 + \tilde{p}_2 = \frac{n}{2}\log_2(M) + 2\lfloor \log_2 \binom{n}{n/2} \rfloor, \tag{5}$$

bits are transmitted per subblock. At the receiver, ML detection in (4) is exploited to detect symbols and indices.

For simplicity, we ignore the effect of CP on spectral efficiency. Then, the spectral efficiencies of OFDM-PIM and OFDM-I/Q-PIM are obtained as $\eta = pG/N$ and $\eta = \tilde{p}G/N$, respectively.

Performance analyses: Since error performance is identical for all subblocks, the pairwise error probability (PEP) events of a single subblock are investigated. Assume that $\mathbf{Z} = \mathrm{diag}(\mathbf{z})$ is transmitted and $\hat{\mathbf{Z}} = \mathrm{diag}(\hat{\mathbf{z}})$ is erroneously detected. Note that from (3), conditional pairwise error probability (CPEP) is given as:

$$\mathrm{P}(\mathbf{Z} \to \hat{\mathbf{Z}}|\mathbf{h}_g) = Q\left(\sqrt{\frac{\Delta}{2N_0}}\right), \tag{6}$$

where $\Delta = ||(\mathbf{Z}-\hat{\mathbf{Z}})\mathbf{h}_g||_F^2 = \mathbf{h}_g^{\mathrm{H}}\mathbf{A}\mathbf{h}_g$ and $\mathbf{A} = (\mathbf{Z}-\hat{\mathbf{Z}})^{\mathrm{H}}(\mathbf{Z}-\hat{\mathbf{Z}})$, $(\cdot)^{\mathrm{H}}$ and $||\cdot||_F$ denote Hermitian transposition and Frobenius norm, respectively. By employing the approximation $Q(x) \approx \frac{1}{12}e^{-x^2/2} + \frac{1}{4}e^{-2x^2/3}$, the unconditional PEP (UPEP) of the OFDM-PIM scheme can be given as in [3]:

$$\mathrm{P}(\mathbf{Z} \to \hat{\mathbf{Z}}) = E_{\mathbf{h}_g}\{\mathrm{P}(\mathbf{Z} \to \hat{\mathbf{Z}}|\mathbf{h}_g)\} \tag{7}$$

$$\approx \frac{1/12}{\det(\mathbf{I}_n + \lambda_1\mathbf{A})} + \frac{1/4}{\det(\mathbf{I}_n + \lambda_2\mathbf{A})}, \tag{8}$$

where $\lambda_1 = 1/(4N_0)$ and $\lambda_2 = 1/(3N_0)$. Finally, the average bit error probability (ABEP) of OFDM-PIM can be upper bounded by

$$\mathrm{P}_b \le \frac{1}{p2^p}\sum_{\mathbf{Z}}\sum_{\hat{\mathbf{Z}}}\mathrm{P}(\mathbf{Z} \to \hat{\mathbf{Z}})e(\mathbf{Z}, \hat{\mathbf{Z}}), \tag{9}$$

where $e(\mathbf{Z}, \hat{\mathbf{Z}})$ is the number of faulty bits for the corresponding error event.

Power level selection strategy: Let $P_1 = 2 - P$, $P_2 = P$, $2 - P > P$ and $1 > P \ge 0$. Therefore, we have only one variable for power level. Note that $\mathbf{Z}$ and P_b are functions of P. In this section, we find the minimum P_b by searching $\sqrt{P}$ values from 0 to 0.99 with increments 0.01. As seen from Fig. 3, the optimum value of $\sqrt{P}$ is obtained as 0.43, 0.47, and 0.6 for $M = 4$, 8, and 16, respectively, with the given parameter $n = 2$ for a fixed SNR of 40 dB. When $P = 0$, it becomes a specific case of OFDM-PIM and equivalent to OFDM-IM with $k = n/2$. When $P = 1$, OFDM-PIM based schemes cannot operate since subcarrier indices become indistinguishable.

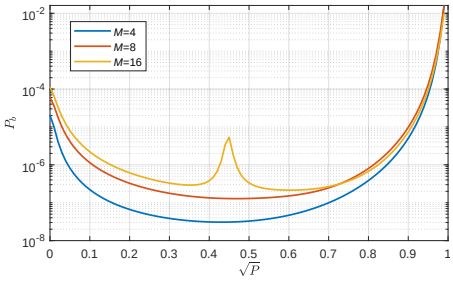

Fig. 3 *Optimum $\sqrt{P}$ search for $n = 2$, varying M, and a fixed SNR of 40 dB.*

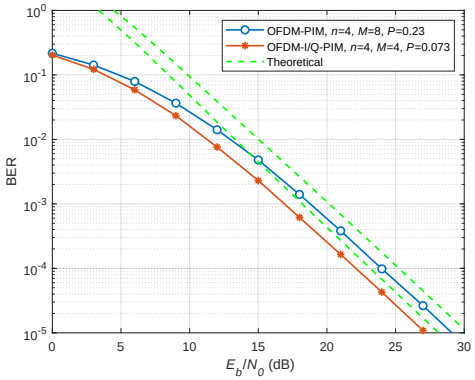

Fig. 4 *Theoretical BER upper bound of OFDM-PIM and OFDM-I/Q-PIM with simulation results for 2 bps/Hz.*

Diversity Order: To prove the diversity order of OFDM-PIM, we investigate the following two cases:

1 Erroneous detection of index bits.
2 Erroneous detection of a single or multiple data symbols when index bits are decoded correctly.

For the first case, due to the inherent feature of IM, $r \ge 2$ is always obtained, where $r = \mathrm{rank}(\mathbf{A})$ determines the diversity order of the system. For example, with $n = 4$, assume that $\mathbf{i} = [1, 3]$ is chosen, however; $\hat{\mathbf{i}} = [2, 3]$ is erroneously decoded. This is the worst case error event since $\mathbf{i}$ and $\hat{\mathbf{i}}$ overlap. We have $r = 2$ even in this error event as in classical OFDM-IM [3]. For the second case, we investigate the following example. For the given parameters $n = 4$, $M = 2$, and $P = 0.073$, assume that $\mathbf{Z}$ with $\mathbf{i} = [3, 4]$, $\mathbf{k} = [1, 2]$ and $\mathbf{x} = [-1, -1]$, is transmitted, neverthless; $\hat{\mathbf{Z}}$ with $\hat{\mathbf{i}} = [3, 4]$, $\hat{\mathbf{k}} = [1, 2]$ and $\hat{\mathbf{x}} = [-1, 1]$, is erroneously decoded. In this case, we have:

$$\mathbf{A} = \begin{bmatrix} 0 & 0 & 0 & 0 \\ 0 & 0.2916 & 0 & 0 \\ 0 & 0 & 0 & 0 \\ 0 & 0 & 0 & 7.7084 \end{bmatrix}, \tag{10}$$

thus, we obtain $r = 2$. As in RC-OFDM, the distribution of the data symbols over multiple subcarriers provides diversity order of 2 even for a single symbol decoding error. It can be deduced that we always obtain $r \ge 2$ for all error events of this type. Consequently, according to the discussion above, we have

$$\min_{\mathbf{Z},\hat{\mathbf{Z}}} \mathrm{rank}(\mathbf{A}) = 2, \tag{11}$$

which shows that OFDM-PIM provides a diversity order of 2. OFDM-I/Q-PIM also provides the same diversity order in a similar manner.

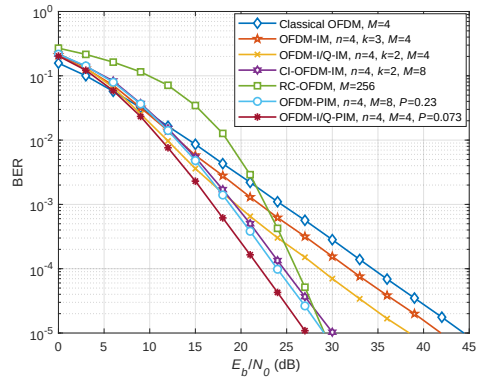

Fig. 5 *Error performance comparison of OFDM-PIM and OFDM-I/Q-PIM with OFDM, RC-OFDM, and CI-OFDM-IM for* 2 *bps/Hz.*

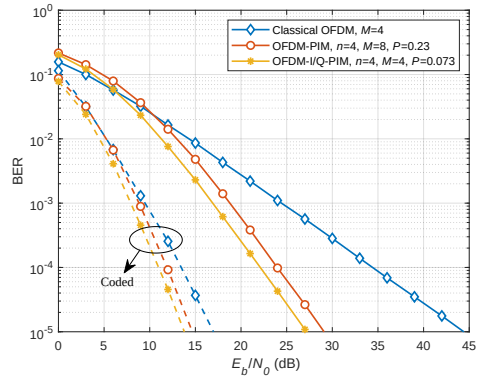

Fig. 6 *Uncoded/Uncoded error performance comparison of OFDM-PIM and OFDM-I/Q-PIM with OFDM.*

Simulation results: In this section, we present computer simulation results to compare the error performance of OFDM-PIM and OFDM-I/Q-PIM with OFDM, RC-OFDM, and various OFDM-IM based schemes. The system parameters are considered as: $N = 128$, $T = 10$, and $C = 16$. For OFDM-PIM and OFDM-I/Q-PIM, the optimum P is obtained by the power level selection strategy discussed previously for a fixed SNR value of 40 dB.

As seen from Fig. 4, theoretical curves obtained by (9) behave as upper bounds for OFDM-PIM and OFDM-I/Q-PIM. Moreover, OFDM-I/Q-PIM provides a 2 dB gain over OFDM-PIM at a bit error rate (BER) value of 10^{-5} due to lower order modulation.

In Fig. 5, we compare the error performance of OFDM-PIM and OFDM-I/Q-PIM with classical OFDM, OFDM-IM, CI-OFDM-IM, OFDM-I/Q/IM, and RC-OFDM. The repetition rate of RC-OFDM is equal to $n = 4$. As seen from Fig. 5, OFDM-PIM and OFDM-I/Q-PIM provide remarkably better error performance than other schemes. At a BER value of 10^{-5}, OFDM-PIM provides nearly the same error performance with RC-OFDM, however; OFDM-I/Q-PIM achieves a 2 dB gain over RC-OFDM. As spectral efficiency increases, RC-OFDM requires a very high modulation order, therefore; the error performance difference between OFDM-PIM-based schemes and RC-OFDM further increases.

Fig. 6 shows the error performance of OFDM, OFDM-PIM, and OFDM-I/Q-PIM with and without 1/3 rate LTE convolutional coding [9]. At a BER value of 10^{-5}, OFDM-PIM and OFDM-I/Q-PIM achieve approximately a 15 dB and 17 dB gain over uncoded-OFDM, respectively. In addition, in the presence of coding, OFDM-PIM and OFDM-I/Q-PIM achieve almost a 2 dB and 3 dB gain over OFDM, respectively. Due to their outstanding error performance, OFDM-PIM-based schemes with coding can be seen as competitive rivals to coded-OFDM which is used in many standards such as IEEE 802.11x.

In Fig. 7, we compare the error performance of OFDM-PIM to RC-OFDM for varying spectral efficiencies. The repetition rate of RC-OFDM is equal to $n = 2$. As seen from Fig. 7, the error performance difference

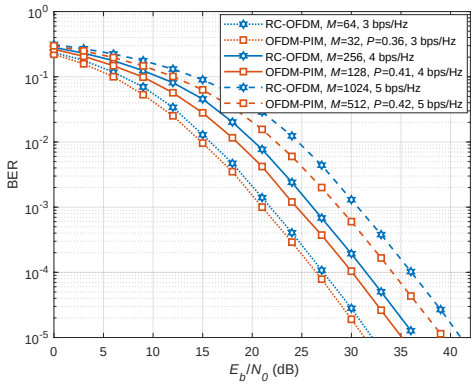

Fig. 7 *Error performance comparison of OFDM-PIM with RC-OFDM for* 3, 4, *and* 5 *bps/Hz when* $n = 2$.

betweeen OFDM-PIM and RC-OFDM increases with increasing spectral efficiency. Moreover, OFDM-PIM can achieve significantly high spectral efficiency rates with acceptable SNR values.

Conclusion: In this letter, we have proposed a novel OFDM-IM based scheme called OFDM-PIM. In OFDM-PIM, we enhance the error performance by applying power distribution to the subcarrier indices of conventional OFDM-IM. OFDM-I/Q-PIM is proposed by extending OFDM-PIM to in-phase and quadrature dimensions to further increase the number of index bits transmitted. The practical implementation of OFDM-PIM and OFDM-I/Q-PIM by employing software definded radios (SDRs) is possible, however; left as future study. OFDM-PIM based schemes can be considered as potential waveforms for 5G and beyond wireless communication systems due to their superior features such as remarkable error performance, simple and flexible transciever structure, diversity gain, and high spectral efficiencies.

Acknowledgment: This work was supported by the Scientific and Technological Research Council of Turkey (TÜBİTAK) under Grant 218E035.

A. T. Dogukan and E. Basar (*Communications Research and Innovation Laboratory (CoreLab), Department of Electrical and Electronics Engineering, Koç University, Sariyer 34450, Istanbul, Turkey.*)

✉ E-mail: ebasar@ku.edu.tr

References

1 F. Sasamori, Z. Jia, S. Handa, and S. Oshita, "Performance analysis of repetition coded OFDM systems with diversity combining and higher-level modulation," *IEICE Trans. Commun.*, vol. 94, no. 1, pp. 194–202, Jan. 2011.
2 E. Basar, "Index modulation techniques for 5G wireless networks," *IEEE Commun. Mag.*, vol. 54, no. 7, pp. 168–175, Jul. 2016.
3 E. Basar, Ü. Aygölü, E. Panayırcı, and H. V. Poor, "Orthogonal frequency division multiplexing with index modulation," *IEEE Trans. Signal Process.*, vol. 61, no. 22, pp. 5536–5549, Nov. 2013.
4 E. Basar, "OFDM with index modulation using coordinate interleaving," *IEEE Wireless Commun. Lett.*, vol. 4, no. 4, pp. 381–384, Aug. 2015.
5 R. Fan, Y. J. Yu, and Y. L. Guan, "Generalization of orthogonal frequency division multiplexing with index modulation," *IEEE Trans. Wireless Commun.*, vol. 14, no. 10, pp. 5350–5359, 2015.
6 E. Arslan, A. T. Dogukan, and E. Basar, "Sparse-encoded codebook index modulation," *IEEE Trans. Veh. Technol.*, pp. 1–1, May. 2020.
7 T. Mao, Z. Wang, Q. Wang, S. Chen, and L. Hanzo, "Dual-mode index modulation aided OFDM," *IEEE Access*, vol. 5, pp. 50–60, Feb. 2017.
8 M. Wen, E. Basar, Q. Li, B. Zheng, and M. Zhang, "Multiple-mode orthogonal frequency division multiplexing with index modulation," *IEEE Trans. Commun.*, vol. 65, no. 9, pp. 3892–3906, Sep. 2017.
9 S. Ahmadi, *LTE-Advanced: A Practical Systems Approach to Understanding the 3GPP LTE Releases 10 and 11 Radio Access Technologies*. New York, NY, USA: Academic, 2014.